

“The inability to image Cherenkov radiation in a conventional radiation treatment environment where room light is on raises significant concern for patient and physician compliance; however, the intensified CCD (ICCD) camera system presented here offers a better solution.”

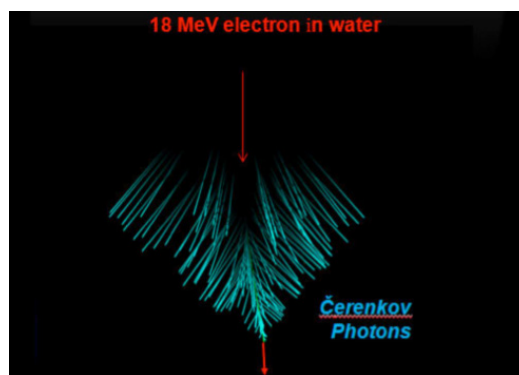
Figure 1.

*Cherenkov photons from one electron.
Image courtesy of Rongxiao Zhang
(Dartmouth College).*

Cherenkov Emission Imaging and Spectroscopy Utilizing Isotopes and a Linear Accelerator

Introduction

Cherenkov radiation, also referred to as either Čerenkov or Cerenkov radiation, takes place when charged particles (e.g., electrons) move through a dielectric (i.e., electrically polarizable) medium at a phase velocity greater than the speed of light in that medium¹. Emission of this radiation (see Figure 1) occurs as the charged particles lose energy inelastically via electric field interactions with the transiently polarized medium².

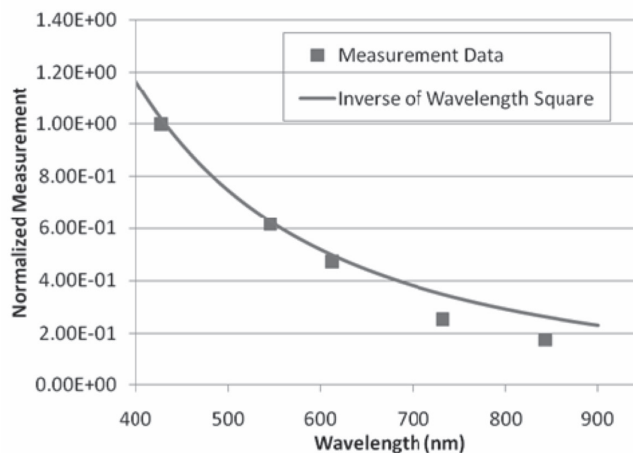


As opposed to fluorescence emission spectra, which have characteristic spectral peaks corresponding to quantized energy transitions, Cherenkov radiation is continuous³. In the visible portion of the spectrum, its relative intensity per unit frequency is proportional to the frequency (as shown in Figure 2)⁴. Thus, because this emission is more intense at higher frequencies (i.e., shorter wavelengths), visible Cherenkov radiation is observed as a brilliant blue³. Note that most Cherenkov radiation, however, is actually in the UV portion of the spectrum. Only with sufficiently accelerated charges does it even become visible.

Recently, it has been shown that radiation from a linear accelerator, or a LINAC (6 to 24 MeV energy), induces Cherenkov radiation emission in tissue, which produces biochemical spectral signatures — this information can be used to estimate tissue hemoglobin and oxygen saturation or molecular fluorescence from reporters⁵. During radiotherapy, spectral absorption features appearing in the Cherenkov radiation emission spectrum can be utilized to quantify blood oxygen saturation (StO₂) from the known absorptions of hemoglobin².

Figure 2.

Results from a series of filtered scans on the wavelength of light detected from positron-emitter samples⁴. The majority of the light is produced in the blue portion of the spectrum, which is expected for Cherenkov radiation, and follows an inverse relationship with the square of the wavelength. Cherenkov light extends into the green and red regions of the EM spectrum, which could increase the range of applications for in vivo imaging studies.



It has also been demonstrated that isotopic β -emitters (^{18}F , ^{11}C , and ^{13}N , with energy <1 MeV) generate Cherenkov emission^{3,6,7}, which is known to be used for optical molecular imaging in small animals.

The most commonly used tracer is the ^{18}F -labeled analog of glucose, 2'-deoxy-2'-[^{18}F] fluoro-D-glucose, or FDG⁴. Metabolically active cells (e.g., in the brain, heart, or malignant tumors) are glucose hungry and therefore accumulate FDG at a higher rate than other tissues⁸. As a marker of cellular glucose consumption and metabolic rate, FDG is employed to assess cancer patients, locate metastatic lesions with higher sensitivity than anatomical imaging modes, and monitor therapeutic response⁹⁻¹¹.

The Cherenkov visible photon yield with high-energy particles exhibits exponential dependence; its optical emission per particle with a higher-energy beam (i.e., from a LINAC) is approximately 2 to 3 orders of magnitude greater compared to the emission from isotopic β -emitters⁵. Hence, LINAC-based optical molecular imaging is now generating considerable interest for clinical disease treatment and monitoring research, whereas isotopic β -emitters are typically employed for the imaging of small animals (in which far less depth is required).

Clinical Disease Treatment in Human Patients

Until now, Cherenkov emission spectroscopy (CES) studies have been done with constant wavelength (CW) signal collection in the absence of ambient lighting^{12,13}, similar to the isotopic β -emitters-based small-animal imaging method, using conventional CCD or EMCCD detectors — although this technique would prevent use on patients because of the concerns of both patient and physician compliance⁵.

Commercial incandescent lights have an irradiance of 10^{-1} to 10^{-3} W/cm², while Cherenkov emission irradiances from a LINAC or a positron emission tomography (PET) agent are approximately 10^{-6} to 10^{-9} W/cm² and 10^{-8} to 10^{-12} W/cm², respectively, depending directly upon dose rate of irradiation⁵. Such large differences in optical irradiance make CW detection

APPLICATION NOTE

of Cherenkov radiation impossible in the presence of ambient light — PET-agent CES works by imaging in a closed environment with a nearly complete absence of light⁵.

New Direction

As it turns out, there are LINACs employed in radiation oncology that produce radiation in pulsed microseconds-long bursts, generated by the accelerator waveguide⁵. Therefore, by taking advantage of a LINAC's inherent pulsed operation, time-gated detection of Cherenkov radiation is possible, significantly improving the ratio of signal to ambient light⁵.

Recently, a research group at Dartmouth College and Dartmouth-Hitchcock Medical Center in New Hampshire led by Dr. Brian Pogue has investigated fluorescence and absorption spectroscopy methods using pulsed LINAC-induced CES^{2,5} under ambient room lighting conditions. An overview of some of their work is provided in the following sections.

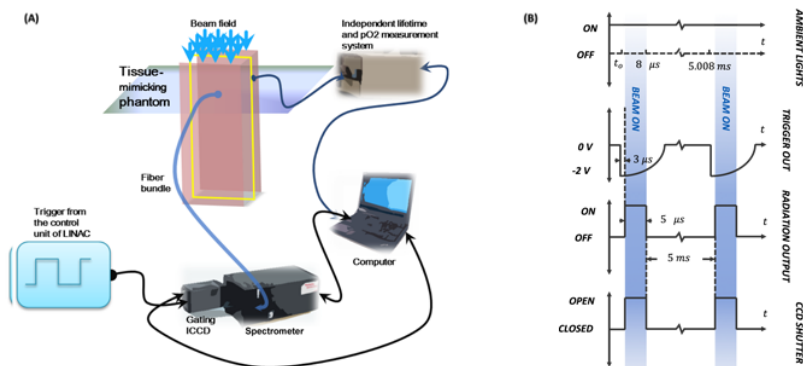
Experimental Setup

In the Dartmouth studies, optical spectra from a phantom were detected using an imaging spectrograph (a SpectraPro[®] 300 from Princeton Instruments) equipped with a 300 lines/mm grating blazed at 750 nm and connected to a front-illuminated ICCD camera (a PI-MAX[®]3:RB from Princeton Instruments) that was configured with a Gen II image intensifier and cooled to -25°C . The optical detection system was placed outside the treatment room and light was collected using a 13 m fiber bundle (Zlight, Latvia) comprising seven 400 μm diameter silica fibers in a hexagonal tip geometry (see Figure 3A)⁵.

For each experiment, the fiber tip was placed in the center of the radiation beam at the phantom surface. A trigger-out voltage was obtained from the LINAC control unit and fed into the external trigger port of the ICCD camera using a BNC cable. In an iterative manner, the delay between the falling edge of the trigger signal and the rising edge of the LINAC beam on pulse was found to be 5 μs . The trigger delay, gate width, and frequency were used in conjunction with Princeton Instruments LightField[®] software to ensure accurate gating and signal acquisition from the spectrometer-ICCD-coupled system (see Figure 3B)⁵.

Figure 3.

The geometry of the measurement system and the temporal acquisition process are shown with (A) the fast time-gated spectrometer system² as well as (B) the timeline⁵ of how the linear accelerator works in pulsed mode and the way to measure decays of Cherenkov radiation emission and excited luminescence (CREL). Diagram and data courtesy of Brian Pogue (Dartmouth College).



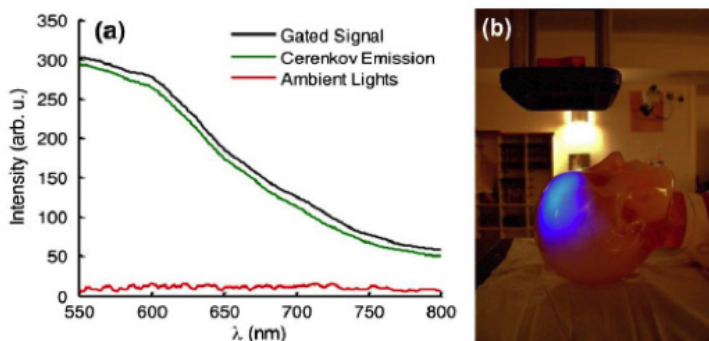
APPLICATION NOTE

Figure 4.

(a) The gated detection of Cherenkov emission with room lights on is shown with spectra acquired from a scattering phantom. The Cherenkov emission is obtained by calculating the difference between the gated signal and ambient lighting signal⁵. (b) A photograph of the room with a corresponding image of Cherenkov emission from a human head phantom for radiation therapy are overlaid to illustrate the amount of ambient lighting present for all experiments⁵. Data and photograph courtesy of Brian Pogue (Dartmouth College).

Results

The group explains that the gated signal spectrum was triggered externally by the LINAC with the beam and ambient lights on. Similarly, the ambient lights spectrum was triggered internally with the beam off and gating parameters identical to that of the gated signal. Isolation of the Cherenkov emission signal was obtained by calculating the difference between the two (see Figure 4). All spectra were subject to background subtraction in order to account for characteristic system noise buildup at the high 100/100x gain⁵.



The Dartmouth researchers relate that the benefit of such a system can be realized when considering the importance of tumor oxygenation in the outcome of external beam radiotherapy (EBRT), as studies have shown hypoxic tumors to be less responsive to treatment due to inadequate damage to tumor DNA^{14,15}. Additional clinical studies have also correlated tissue oxygen pressure (pO_2) to EBRT effect in head and neck cancers and suggested that pO_2 increases during fractionated treatment plans^{16,17}. Therefore, there is great potential value in a noninvasive technique, such as CES, for monitoring tumor oxygen saturation during EBRT⁵.

The group emphasizes that the inability to make measurements in a conventional radiation treatment environment where ambient room light is always present raises significant concern for patient and physician compliance; however, the gated ICCD camera system presented here offers a better solution to this problem via $\sim 1000x$ reduction in ambient light contribution to the CES signal when the radiation is gated, such as with a LINAC⁵.

Additional Comments

To monitor clinical disease treatment in human patients using Cherenkov emission spectroscopy with a linear accelerator, a gated ICCD camera such as the Princeton Instruments PI-MAX4:1024i-HR represents an excellent choice (see Figure 5).

APPLICATION NOTE

Figure 5.

The PI-MAX4:1024i-HR gated ICCD camera from Princeton Instruments.



It is worth noting that because small-animal imaging can be conducted in a dark environment (i.e., with a dark box) and utilizes isotopic β -emitters, which inherently have 2 to 3 orders of magnitude less visible light yield, a higher-sensitivity, electron-multiplying ICCD (*eml*CCD) camera such as the Princeton Instruments PI-MAX4:512EM* can be utilized instead of a traditional ICCD camera.

Resources

To learn more about the research being conducted at Dartmouth, please visit:

<http://engineering.dartmouth.edu/people/faculty/brian-pogue/>

For additional information about Princeton Instruments ICCD and *eml*CCD cameras, please visit: <http://www.pi-max4.com>

References

1. P.A. Cherenkov, *C.R. Acad. Sci. URSS* 20, 651–655 (1938).
2. R. Zhang, A. Glaser, T.V. Esipova, S.C. Kanick, S.C. Davis, S. Vinogradov, D. Gladstone, and B. Pogue, *Biomed. Opt. Express*. 3(10), 2381–2394 (2012).
3. J.V. Jelley, *Br. J. Appl. Phys.* 6(7), 227–232 (1955).
4. R. Robertson, M.S. Germanos, C. Li, G.S. Mitchell, S.R. Cherry, and M.D. Silva, *Phys. Med. Biol.* 54, N355 (2009). [Author manuscript cited; available via NIH Public Access.]
5. A.K. Glaser, R. Zhang, S.C. Davis, D.J. Gladstone, and B.W. Pogue, *Opt. Lett.* 37(7), 1193–1195 (2012).
6. S.M. Ametamey, M. Honer, and P.A. Schubiger, *Chem. Rev.* 108, 1501–1516 (2008).
7. H.H. Ross, *Anal. Chem.* 41, 1260–1265 (1969).
8. O. Warburg, *Science* 123, 309–314 (1956). [PubMed: 13298683]

APPLICATION NOTE

9. G.J. Kelloff, J.M. Hoffman, B. Johnson, H.I. Scher, B.A. Siegel, E.Y. Cheng, B.D. Cheson, J. O'Shaughnessy, K.Z. Guyton, M.A. Mankoff, L. Shankar, S.M. Larson, C.C. Sigman, R.L. Schilsky, and D.C. Sullivan, *Clin. Cancer Res.* 11, 2785–2808 (2005). [PubMed: 15837727]
10. N.G. Mikhaeel, M. Hutchings, P.A. Fields, M.J. O'Doherty, and A.R. Timothy, *Ann. Oncol.* 16, 1514–1523 (2005). [PubMed: 15980161]
11. L.K. Shankar, J.M. Hoffman, S. Bacharach, M.M. Graham, J. Karp, A.A. Lammertsma, S. Larson, D.A. Mankoff, B.A. Siegel, A. Van den Abbeele, J. Yap, and D. Sullivan, *J. Nucl. Med.* 47, 1059–1066 (2006). [PubMed: 16741317]
12. J. Axelsson, S.C. Davis, D.J. Gladstone, and B.W. Pogue, *Med. Phys.* 38(7), 4127 (2011).
13. J. Axelsson, A.K. Glaser, D.J. Gladstone, and B.W. Pogue, *Opt. Express* 20, 5133 (2012).
14. P. Vaupel, A. Mayer, and M. Höckel in *Recombinant Human Erythropoietin (rhEPO) in Clinical Oncology*, M. R. Nowrousian, eds. (Springer, 2008) pp. 265–282.
15. S.M. Evans and C.J. Koch, *Cancer Lett.* 195, 1 (2003).
16. M. Nordmark, S.M. Bentzen, V. Rudat, D. Brizel, E. Lartigau, P. Stadler, A. Becker, M. Adam, M. Molls, J. Dunst, D.J. Terris, and J. Overgaard, *Radiother. Oncol.* 77, 18 (2005).
17. R.A. Cooper, C.M. West, J.P. Logue, S.E. Davidson, A. Miller, S. Roberts, I.J. Stafford, D.J. Honess, and R.D. Hunter, *Int. J. Radiat. Oncol. Biol. Phys.* 45, 119 (1999).
18. R. Zhang, D.J. Gladstone, L.A. Jarvis, R.R. Strawbridge, P. Jack Hoopes, O.D. Friedman, A.K. Glaser, and B.W. Pogue, "Real-time in vivo Cherenkov imaging during external beam radiation therapy," *J. Biomed. Opt.* 2013 Nov; 18(11): 110504.
19. Lesley A. Jarvis, Rongxiao Zhang, David J. Gladstone, Shudong Jiang, Whitney Hitchcock, Oscar D. Friedman, Adam K. Glaser, Michael Jermyn, and Brian W. Pogue, "Cherenkov video imaging allows for the first visualization of radiation therapy in real time" *Int. J. Radiation Oncology, Biology & Physics* (in press, 2014).

*Please note that all PI-MAX4 cameras with a Gen III image intensifier or an EMCCD require an end-user statement and licensing process for shipments outside the United States.

APPLICATION NOTE